

The Crystallization and Morphology of Biodegradable Poly(butylene succinate-*co*-terephthalate) Copolyesters with High Content of BT Units

Faxue Li,^{1,2} Shengli Luo,^{1,2} Chi Ma,^{1,2} Jianyong Yu,³ Amin Cao⁴

¹Key Laboratory of Textile Science & Technology, Ministry of Education, Donghua University, Shanghai 201620, P.R. China

²College of Textile, Donghua University, 2999 North Renmin Road, Shanghai 201620, P.R. China

³Modern Textile Institute, Donghua University, Shanghai 200051, P.R. China

⁴Laboratory for Polymer Materials, Shanghai Institute of Organic Chemistry, Chinese Academy of Sciences, 354 Fenglin Road, Shanghai 200032, P.R. China

Received 26 September 2008; accepted 28 February 2010

DOI 10.1002/app.32381

Published online 24 May 2010 in Wiley InterScience (www.interscience.wiley.com).

ABSTRACT: Isothermal crystallization and morphology of biodegradable PBST copolyesters with high content of BT units were investigated. The crystallization kinetic analysis showed that the Avrami exponent n ranged from 3.2 to 4.9, indicating a three-dimensional growth initiated by homogeneous nucleation mechanism at low crystallization temperature and heterogeneous nucleation mechanism at high temperature. After isothermal crystallization, multiple melting peaks were observed during DSC heating, and were explained by the melting and recrystallization model. The equilibrium melting temperatures of the PBST copolyesters were determined by Hoffman–Weeks and Gibbs–Thomson methods, respectively. Two methods, however, gave differ-

ent values for each sample. The origin of the complexity and its influences on the equilibrium melting temperature of the copolyesters were analyzed. According to WAXD measurement, the copolyesters were identified to have the same crystal structure as that of PBT, suggesting that only the BT units were crystallized in the system whereas the BS units were in the amorphous state. POM micrographs showed that the crystals of the copolyesters were composed of little spherulites, beneficial to forming flexible fibers. © 2010 Wiley Periodicals, Inc. *J Appl Polym Sci* 118: 623–630, 2010

Key words: poly(butylene succinate-*co*-terephthalate); crystallization kinetics; Avrami equation; morphology

INTRODUCTION

Aliphatic polyesters are one of the most promising structural materials for biodegradable or compostable copolyesters forming nonwovens, films, sheets, bottles, and injection-molded products. However, commercial high molecular weight aliphatic polyesters have been limited to polyesters produced by either microorganisms,¹ ring-opening polymerization of lactones,² or ring-opening polyaddition of cyclic dimers,³ resulting in high production costs and inherent poor physical and mechanical properties. On the other hand, poly(butylene succinate) (PBS), produced through polymerization of succinic acid and 1,4-butanediol, is known to be an excellent biodegradable polymer with high melting temperature and mechanical strength, and consequently, many

improved copolymers based on PBS have been reported.^{4–7}

Meanwhile, aromatic polyesters are materials displaying an excellent array of physical properties. As they are strongly resistant to hydrolysis as well as to bacterial and fungal attack, they usually remain in environment for prolonged time without significant loss of the properties. Therefore, the combination of aliphatic and aromatic units in the same polyester chain has been envisaged for a long time as an attractive approach to obtain novel products encompassing biodegradability and good mechanical properties. Poly(butylene adipate-*co*-terephthalate)s (PBAT, Ecoflex[®]) are such a commercialized aliphatic–aromatic biodegradable copolymer from BASF. Their thermal, mechanical, and biodegradable properties were reported by Müller and coworkers.^{8–10} Based on these researches, the aliphatic–aromatic copolyesters with aromatic units within the range of 35–55 mol % offer an optimal balance between its biodegradability and physical properties.

In our previous work, we developed poly(butylene succinate-*co*-terephthalate) (PBST) copolyesters, similar to PBAT in chemical structure, and conducted some investigation on their biodegradation property.¹¹ The results indicated that the degradation still

Correspondence to: F. Li (fxlee@dhu.edu.cn).

Contract grant sponsor: Programme of Introducing Talents of Discipline to Universities; contract grant number: B07024.

TABLE I
The Properties of the Synthesized PBST Copolyesters with High BT Unit Content

Sample	Composition		Molecular weight ^a			Thermal properties			
	Feed ratio T/S ^b	Unit ratio BT/BS ^c	$M_w/\times 10^{-4}$	$M_n/\times 10^{-4}$	M_w/M_n	T_m^d (°C)	T_c^d (°C)	ΔH^d (J/g)	T_m^0 ^e (°C)
PBST-50	50 : 50	55 : 45	20.16	8.69	2.32	138.0	120.7	35.18	176
PBST-60	60 : 40	62 : 38	24.28	8.88	2.74	163.3	138.6	40.25	185.4
PBST-70	70 : 30	71 : 29	14.35	4.60	3.12	180.0	150.5	49.37	194.4

^a The values were evaluated by ¹H-NMR.

^b Molecular weights were measured by GPC. Polystyrene was used to calibrate the elution traces.

^c The values indicated feeding molar ratio of DMT to DMS.

^d The melting temperature T_m , crystallization temperature T_c , and melting enthalpy ΔH were measured by DSC.

^e The values of equilibrium melting temperature were calculated by Gibbs–Thomson method.

happened to PBST copolyesters with BT unit content of 70 mol %, although the degradation rate decreased with increasing BT unit contents.

Generally, the biodegradable aliphatic–aromatic copolyesters reported so far were those bearing low content of aromatic units. These polymers tended to be associated with low melting temperature and were unsuitable for manufacturing textile fibers. Therefore, in this article, we first prepared PBST copolyesters with high content of aromatic units, and then investigated their properties for fiber formation. It is worth pointing out that the PBST fibers, especially prepared at low take-up velocity, have rubbery-like stress–strain curves of good elasticity. They exhibit low modulus, moderate tensile strength but high elongation at break. In addition, good recoverability of the PBST fibers was also observed in cyclic deformation test. Details on the elastic property of PBST fibers and its mechanism will be reported in a separate article.

It is well-known that the mechanical properties and biodegradation rate of biodegradable polyesters depend strongly on their chemical structure, as well as morphology and crystallinity, which in turn are determined directly by the thermal treatment imposed on the polymers during solidification process. Therefore, it is very important to investigate the crystallization kinetics and morphology of these biodegradable aliphatic–aromatic copolyesters so as to understand the relationship between structural features and crystallization conditions. Thus, this study focused on the isothermal crystallization kinetics and crystallization morphology of the biodegradable PBST copolyesters with high content of BT units to understand the effects of BT units on the crystallization of the copolyesters.

EXPERIMENTAL

Materials

PBST pellets were synthesized via condensation copolymerization strategy from the starting materials of dimethyl terephthalate (DMT), dimethyl succinate

(DMS) and large amount of 1,4-butanediol (1,4-BD). The detailed preparation of these copolyesters was described elsewhere.¹² The feed molar ratio of DMT to DMS was 50 : 50, 60 : 40, and 70 : 30, assigned as PBST-50, PBST-60, and PBST-70, respectively. The molecular weights and molar ratio of butylene succinate (BS) to butylene terephthalate (BT) in copolyesters are shown in Table I, as also other thermal properties. The pellets were carefully dried in a vacuum oven at 50°C for 24 h before melt-pressing into films.

Differential scanning calorimetry measurement

The isothermal crystallization kinetics of PBST copolyesters was analyzed by using a differential scanning calorimeter (PerkinElmer DSC Pyris-1), which was routinely calibrated with indium and zinc. The sample was heated up to a temperature about 20°C above the corresponding melting temperature, remaining for 5 min to eliminate the thermal and mechanical history, and then cooled to the preset crystallization temperature (T_c) at a rate of 200°C/min with liquid nitrogen for isothermal crystallization. The heat generated during the development of the crystalline phase was recorded until no further heat evolution was observed, and analyzed according to the usual procedure to obtain the relative crystallinity (X_t).

After crystallization, the sample was reheated at a heating rate of 10°C/min. The corresponding melting temperature was obtained for investigating the equilibrium melting temperature (T_m^0) of the PBST copolyesters.

X-ray measurement

The X-ray measurement of the melt-crystallized copolyester films was performed at room temperature on a Panalytical X'pert-Pro system. The power of the generator is 40 kV \times 40 mA, and Nickel-filtered Cu K α radiation ($\lambda = 0.154$ nm) is used. The wide angle X-ray diffraction (WAXD) profiles were recorded in the 2 Θ range of 2–50° at a scan rate of

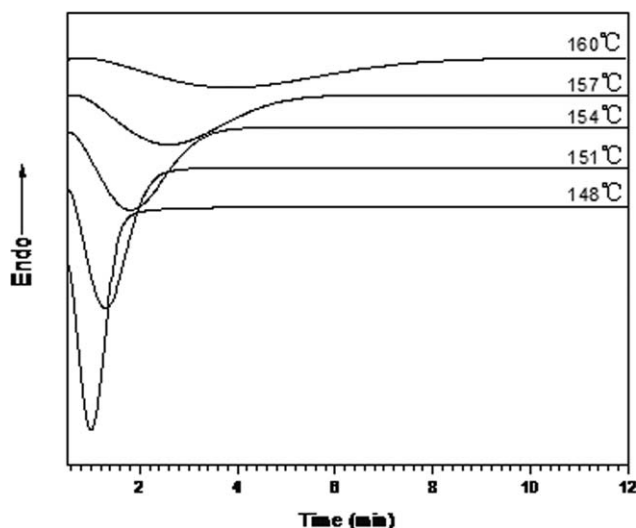


Figure 1 DSC crystallization curves of PBST-70 copolyesters at different temperatures.

0.02°/min. The small angle X-ray scattering (SAXS) experiments of the films isothermally crystallized at various T_c s were conducted on the same system at room temperature. SAXS profiles were recorded in the 2θ range of 0.1–2.0° at a scan rate of 0.01°/min.

Polarized optical microscope measurement

Spherulite morphology was characterized under various crystallization temperatures for PBST copolyesters on an Olympus BX51 polarized optical microscope (POM) with the digital camera of JVC TK-C1380 system and HCS410 thermal stage. First, the sample was sandwiched between two thin glass slides. Then it was heated up beyond its corresponding melting temperature, and kept there for 5 min. Finally, the sample was cooled rapidly with liquid

nitrogen to a predetermined crystallization temperature for crystallization and morphological studies.

RESULTS AND DISCUSSION

Isothermal crystallization of copolyesters

Figure 1 shows the DSC thermograms for PBST-70 at various T_c s. It can be seen that the time at the crystallization exothermic peak is different as T_c varies. With the increase of T_c , the crystallization exothermic peak gradually shifts to longer time and becomes flatter, indicating that the isothermal crystallization process takes more time to approach the final equilibrium state at a higher temperature.

The relative crystallinity (X_t) as a function of crystallization time (t) was given by eq. (1)

$$X_t = \frac{\int_{t_0}^t \left(\frac{dH_t}{dt} \right) dt}{\int_{t_0}^{\infty} \left(\frac{dH_t}{dt} \right) dt} \quad (1)$$

where t_0 is the crystallization induction time, as indicated by a flat baseline after the initial spike in the thermal curve, and dH/dt is the heat flow rate. Figure 2(a) represents the plots of X_t versus t for the sample under various T_c . For the isothermal crystallization, the Avrami equation can be employed to investigate the melt-crystallization kinetics by assuming the development of X_t with t as^{13,14}

$$1 - X_t = \exp(-(K^{1/n}(t - t_0))^n) \quad (2)$$

where K is the isothermal crystallization rate constant and n is the Avrami exponent, which is related to the type of nucleation and the geometry of crystal growth. From the intercepts and the slopes of the plots of $\ln[-\ln(1 - X_t)]$ versus $\ln(t - t_0)$, values of $K^{1/n}$

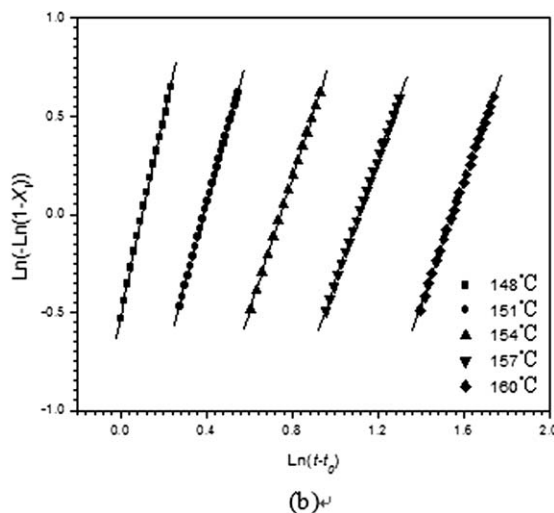
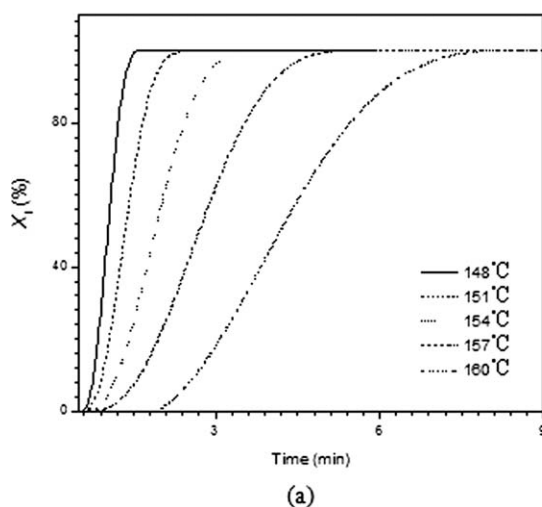


Figure 2 Isothermal crystallization from the melt of PBST-70. (a) Relative crystallinity with crystallization time, (b) Avrami analysis for the sample.

TABLE II
The Parameters of Isothermal Crystallization and Solid Structure of PBST Copolyesters with High BT Unit Content

Sample	T_c (°C)	n^a	$\ln K^{1/n}$ ^a	$t_{1/2}$ ^a (min)	$t_{1/2}$ ^b (min)	T_m^c (°C)	X_c^d (%)	L_p (nm)	l_c (nm)
PBST-50	110	4.2	0.36	0.47	0.48	144.1	25.2	6.8	1.7
	113	4.2	-0.27	0.57	0.59	145.7	25.8	7.0	1.8
	116	3.8	-0.8	0.66	0.68	147.3	26.0	7.3	1.9
	119	3.6	-1.25	0.74	0.77	148.2	26.7	7.4	2.0
	122	3.2	-2.07	1.14	1.18	149.7	27.3	7.6	2.1
PBST-60	133	4.5	0.18	0.63	0.61	162.2	28.9	7.1	2.1
	136	3.9	-0.35	0.85	0.87	163.1	29.3	7.3	2.1
	139	3.7	-0.78	1.12	1.10	164.7	29.8	7.5	2.2
	142	3.8	-1.08	1.82	1.85	165.4	30.5	7.8	2.4
	145	3.3	-1.65	2.15	2.18	166.8	31.6	8.1	2.6
PBST-70	148	4.9	-0.11	1.03	1.05	176.8	35.5	8.7	3.1
	151	4.0	-0.39	1.35	1.35	178.1	36.8	9.4	3.5
	154	3.4	-0.75	1.91	1.88	179.2	37.2	9.8	3.6
	157	3.1	-1.13	2.71	2.70	180.6	38.8	10.1	3.9
	160	3.2	-1.53	4.18	4.20	182.0	39.6	11.2	4.4

^a The values were obtained by the eq. (3).

^b The values were obtained according to the curves of relative crystallinity versus crystallization time such as Figure 2(a).

^c The melting temperature T_m was obtained from the DSC heating curve of PBST copolyesters crystallized isothermally at different temperature.

^d The degree of crystallinity X_c was equal to the ratio of heat of fusion of PBST copolyesters isothermally crystallized at various T_c s to that of perfect crystal, and the heat of fusion of perfect crystal was 144.5 J/g reported in the Ref. 12.

and n can both be calculated. Let $X_t = 0.5$ in eq. (2), crystallization half-time, $t_{1/2}$, defined as the time at which the extent of crystallization is 50%, can be obtained

$$t_{1/2} = \left(\frac{Ln2}{K} \right)^{1/n} \quad (3)$$

Figure 2(b) describes the plots of $\ln[-\ln(1-X_t)]$ versus $\ln(t-t_0)$ of PBST-70 at different T_c s. It can be found that each plot is basically a straight line, indicating the isothermal crystallization of the copolyesters follows the Avrami equation. The values for n , $t_{1/2}$ and $\ln K^{1/n}$ can be determined from the plots and summarized in Table II. In all cases, the values of n are fractional, which can be explained in terms of a partial overlapping of primary nucleation and crystal growth.¹⁵ Furthermore, the exponent n ranges from 3.2 to 4.9, implying three-dimensional spherulitic growth initiated by homogeneous nucleation mechanism is the dominant nucleation mechanism. Generally, the exponent n around 4 is expected for a spherulitic growth and a homogeneous nucleation. In some cases, the high value of the Avrami exponent 4.9 was obtained, which may be caused by the several reasons as follow: the effects of time-dependent initial nucleation, homogeneous nucleation and heterogeneous nucleation existed simultaneously. In addition, the effect of secondary crystallization may be also an important reason. These indicate that the polymer crystallization is much more complex than reflection of Avrami model. Therefore, in despite of various BT unit content in PBST copolyesters, the nucleation mechanism and geometry of crystal

growth remain the same in the temperature range investigated.

On the other hand, it can be seen that, according to Table II, the values of $t_{1/2}$ deduced from Avrami equation increase with increasing the T_c , indicating the crystallization rate decrease with the T_c . To verify the validity of Avrami analysis, the $t_{1/2}$ values obtained by DSC measurement are also listed in the table. It is found that the $t_{1/2}$ values from two methods show a similar variation tendency although they are different from each other, suggesting the Avrami equation is adopted suitably to analyze the isothermal crystallization of PBST copolyesters. Moreover, the values of the crystallization rate $K^{1/n}$ decrease with the increase of T_c . This implies that the melt crystallization of PBST copolyesters exhibits a temperature dependency that is the characteristic of nucleation-controlled crystallization associated with the adjacency of the melting temperature. The decrease of $K^{1/n}$ value is mainly due to the stronger thermal movement of macromolecular chains at higher T_c . The higher crystallization temperature restricts the forming of crystal nuclei, or promotes the instability of crystal nuclei.

As the crystallization is assumed to be thermally activated, the crystallization rate constant K can be approximately described in the Arrhenius form,¹⁶ i.e.

$$\ln K^{1/n} = \ln K_0 + (\Delta E/RT_c) \quad (4)$$

where K_0 is a temperature-independent factor, ΔE is the total crystallization activation energy, R is the

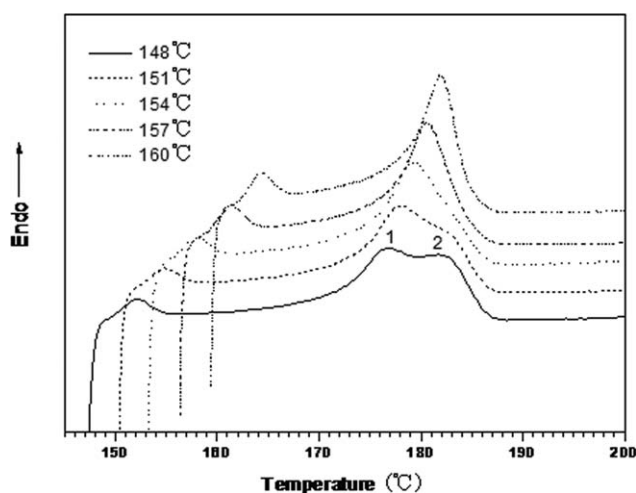


Figure 3 DSC heating curves of PBST-70 crystallized isothermally at different temperatures.

gas constant, and T_c is the absolute temperature. ΔE can be determined by multiplying R with the slope of the linear plot of $\ln K^{1/n}$ versus $1/T_c$, and consists of both the free energy in formation of the critical size nuclei at respective T_c , and the activation energy required for transporting molecular segments across the phase boundary to the crystallization surface. With this technique, the ΔE values of PBST-50, -60, and -70 were calculated as 244.7, 206.3, and 180.5 kJ/mol, respectively, indicating these values increase with the BS unit content. The BS units on the backbone can weaken the structural integrity of the polymer chain and shorten the length of BT segment reported in the previous study.¹²

Multiple melting behavior of copolyesters

Figure 3 depicts the DSC heating curves of PBST-70 after isothermal crystallization at various T_c s. To prevent further crystallization from occurring during cooling process, the sample was heated directly from T_c to melt. It can be observed that the shapes and positions of the endothermic peaks for PBST-70 are influenced by T_c . At lower crystallization temperatures, there are two melting endothermic peaks of 1 and 2. Peak 1 shifts to higher temperature side with increasing T_c , while peak 2 moves in opposite direction until two peaks are merged into a single one.

Many articles have investigated the origination of double melting peaks, and an acceptable opinion is recrystallization.¹⁷ The lower melting peak arises from original crystals, while the higher one results from recrystallization during heating. The fact that polymers crystallize as metastable lamellae is the reason that recrystallization is possible during an elevating temperature scan. The metastable lamellae have lower melting temperatures because of their

large surface/volume ratios and the high surface energy of their folded surfaces. By increasing the thickness/size of the lamellae to allow partially melting and then recrystallizing, a sample can reduce its total free energy. The BS units tend to crystallize themselves or change the crystallization behavior of BT units in some ways. To explore this further, the multiple melting peaks of PBST-70 are studied by varying the heating rate.

Measurements carried out at different heating rates can clarify whether the melting and recrystallization occurs during the melting process of the sample. Figure 4 shows the DSC melting curves of PBST-70 crystallized at 151°C at different heating rates. With the increase of heating rate, the endothermic peak 1 shifts gradually toward higher temperature, whereas the endothermic peak 2 shifts to lower temperature until the two merging into one, and thus the evidences for melting and recrystallization are provided. According to the melting and recrystallization model, the small and imperfect crystals tend to turn successively into more stable crystals with increasing the temperature. At high heating rates, however, the sample passes through the crystallization region so rapidly that there is no sufficient time for the melts to reorganize into new crystals. Hence, the recrystallization process is largely inhibited and the endothermic peak 2 disappears. Furthermore, it is interesting to note that a small melting peak located at about 155°C becomes more apparent with the increasing heating rate, the reason and implication of this peak will be examined in our subsequent research.

Equilibrium melting temperature of copolyesters

Equilibrium melting temperature (T_m^0) is one of the most important parameters for a polymer, and its

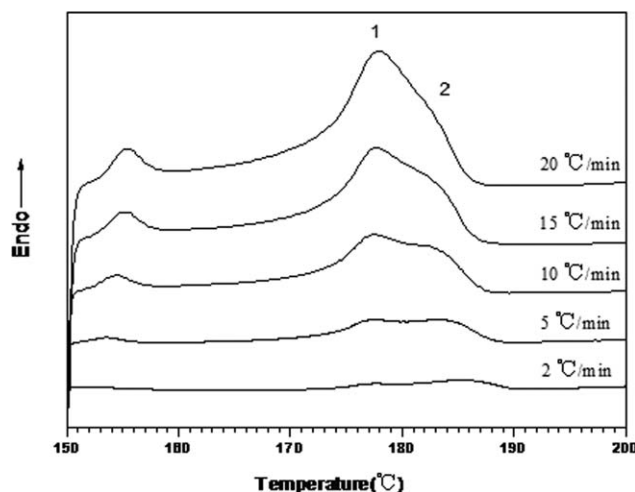


Figure 4 DSC melting curves at different heating rates for PBST-70 crystallized at 151°C.

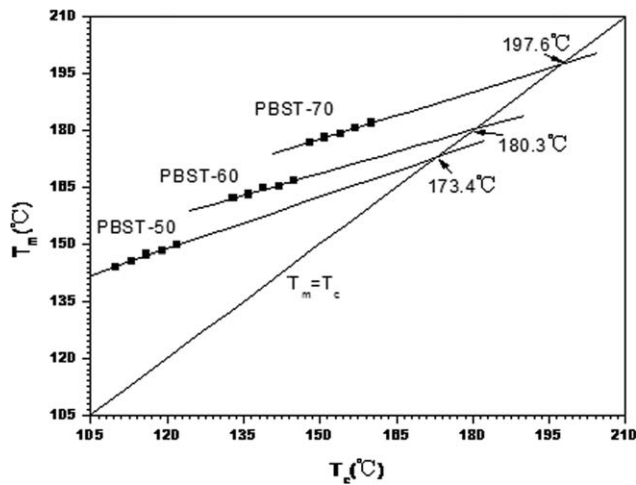


Figure 5 Dependence of observed melting temperatures on crystallization temperatures for melt-crystallized.

precise measurement is a crucial problem in the fundamental study of polymer crystallization. On the basis of the definition, T_m^0 is the melting temperature of lamellar crystals with infinite thickness. In practice, it is impossible to obtain such a thermodynamically stable polymer lamellar crystal. Because of the complex interactions among the kinetic factors during crystallization process, usually chain-folded polymer lamellar crystals with a finite thickness of about 10 nm are resulted. In consideration of the dependence of observed melting temperature T_m on crystallization conditions for a chain-folded polymer, T_m^0 is generally extrapolated from the observed T_m . The extrapolation method depends not only on the kinetic factors and experimental conditions such as metastability of the chain-folded crystals, and heating rate of a crystallized sample, but also on the theory adopted. Therefore, determination of T_m^0 is a complex issue, and even for the same polymer sample, different values of T_m^0 may be obtained by different researchers under different experiment conditions.

The usual theory to determine T_m^0 is called the Hoffman–Weeks equation given as¹⁸

$$T_m = T_m^0 \left(1 - \frac{1}{\xi}\right) + \frac{T_c}{\xi} \quad (5)$$

where ξ is the thickening coefficient. According to this equation, a linear extrapolation curve of observed T_m as a function of T_c intersects the equilibrium line $T_m = T_c$ at an intersection point T_m^0 . So by simply using the DSC method to measure the observed melting temperatures at different T_c s, T_m^0 can thus be determined. Because of the experimental and analytical simplicities, this method has been widely used.

Because melting peak 1 is originated from the lamellae formed at T_c , the T_m^0 of PBST-70 was

obtained from the relationship of T_m at peak 1 and the corresponding T_c . By using the Hoffman–Weeks equation, the linear regression of T_m versus T_c and extrapolation to the line of $T_m = T_c$ shown in Figure 5 indicate that the equilibrium melting temperature T_m^0 of PBST-50, -60, and -70 is 173.4, 180.3, and 197.6°C, respectively.

Another method is the Gibbs–Thomson equation, which is a strict thermodynamic argument that the observed melting temperature T_m of a lamellar crystal with a thickness of l_c is given by¹⁹

$$T_m = T_m^0 \left(1 - \frac{2\sigma_e}{\Delta h_f l_c}\right) \quad (6)$$

where σ_e is the surface free energy used for the chain folding during the crystallization process, and Δh_f is the heat of fusion per unit volume of the crystal. The equation indicates that the observed T_m of a thin lamellar crystal is depressed below that of an infinite crystal by an amount of $2T_m^0\sigma_e/(\Delta h_f l_c)$. Thus, simply plotting T_m versus $1/l_c$, the intercept at $1/l_c \rightarrow 0$ is the equilibrium melting temperature T_m^0 .

The Lorentz-corrected SAXS profiles of PBST-70 films isothermally crystallized at different T_c s are represented in Figure 6, where the scattering vector $q = 4\pi(\sin \Theta)/\lambda$, with 2Θ as the scattering angle, and q^* is the scattering vector corresponding to the peak. The long period or the interlamellar spacing can be calculated from the equation $L_p = 2\pi/q^*$. Moreover, the thickness of the crystal lamellar region (l_c) can be obtained through multiplication of the long period by the degree of crystallinity (X_c), according to Vonk's method,²⁰ as listed in Table II. Figure 7 illustrates the relationship between the inverse lamellar thickness $1/l_c$ and the observed T_m s for PBST-50, -60, and -70. It is shown that good

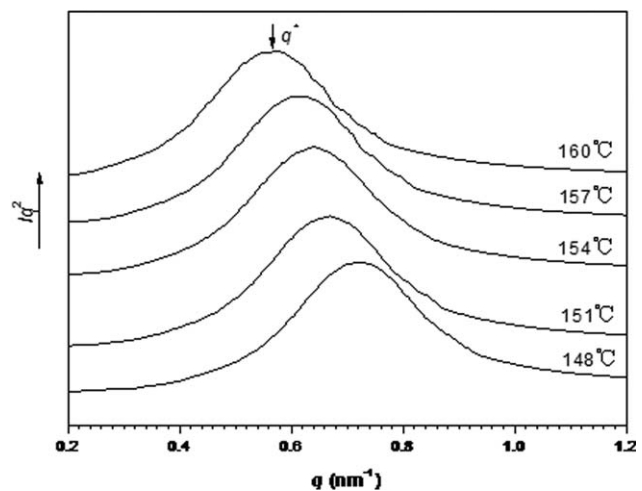


Figure 6 PBST copolyesters. Lorentz-corrected SAXS profiles for PBST-70 films melt-crystallized at different temperatures.

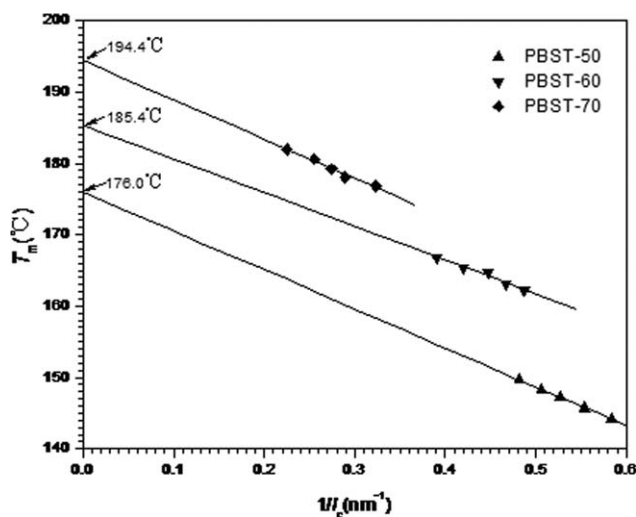


Figure 7 Variation in melting temperature (T_m) as a function of inverse lamellar thickness ($1/l_c$) for melt-crystallized PBST copolyesters.

linear fittings are found between T_m and $1/l_c$, given the experimental errors. The results demonstrate that the experimental data obey the Gibbs–Thomson method, and the equilibrium melting temperature T_m^0 of PBST-50, -60, and -70 is attained for 176.0, 185.4, and 194.4°C respectively, a bit different from those obtained by Hoffman–Week method.

To seek the reason that the T_m^0 s of PBST copolyesters determined by two methods are so different, the origins of the two methods should be reviewed first. The Hoffman–Weeks equation is actually deduced from a combination of the Gibbs–Thomson equation and the secondary nucleation theory.²¹ The prerequisite for its application is the isothermal thickening process of the lamellar crystals at a specific crystallization temperature and the independence of the thickening coefficient ξ on the T_c . Obviously, the lamellar thickening is a complicated kinetic process and is affected by many kinetic factors. Therefore, as pointed out in many articles, it is doubtful that the coefficient ξ would remain a constant during an isothermal crystallization. On the contrary, the coefficient is known to be a complex function not only of supercooling, but also of the polymer chemical structure and the crystalline and amorphous phase structure.^{22–24} Thus, the prediction of T_m^0 simply based on the relationship between T_c and observed T_m is a bit arbitrary, for the Hoffman–Week method merely shows the dependence of observed T_m on the T_c but only provides a rough estimation of T_m^0 .

Crystal structure of copolyesters

Further information on the crystal structure was obtained from WAXD measurement. Figure 8 shows diffraction patterns of the PBST copolyesters with high BT unit content. The sharp diffraction peaks

are indicative of the presence of crystallites in the copolyesters. According to the figure, it can be found that the similar characteristic diffractions are observed for the three samples. The diffraction peaks of the PBST copolyesters at $2\Theta = 16.1^\circ(0\bar{1}1)$, $17.2^\circ(010)$, $20.2^\circ(\bar{1}01)$, $23.2^\circ(100)$, $25.1^\circ(1\bar{1}1)$ agree well with those of poly(butylene terephthalate) (PBT),²⁵ suggesting that the prepared PBST copolyesters have the same crystal structure as the PBT. According to the literature,²⁶ PBS forms a monoclinic crystal lattice with the characteristic diffractions at the 2θ angles of 19.6° , 21.5° , and 22.5° assignable to the (020), (021), and (110) planes, respectively. No appearance of these characteristic diffractions in the WAXD spectra indicates that the added BS unit is in the noncrystalline state as minor components in the copolyesters, although BS unit itself is crystallizable.

Crystallization morphology of copolyesters

Figure 9 displays the POM micrographs of three kinds of PBST copolyesters isothermally crystallized at various temperatures. It can be seen that the crystals of the three samples are composed of little spherulites, which show the well-defined Maltese cross pattern despite different BS unit contents. Based on the WAXD measurement above, the little spherulites should be composed of the BT folded chains, similar to that of PBT homopolymer. Nevertheless, through POM measurements on the PBT film specimens crystallized at three kinds of conditions, Yoshioka et al.²⁷ found that each specimen contained a type of large spherulites. This means that the import of BS units on the backbone of PBT leads to obvious suppressing effect on the crystallization of BT units, although it unalters the triclinic crystal structure. Practically, it is these less stiff

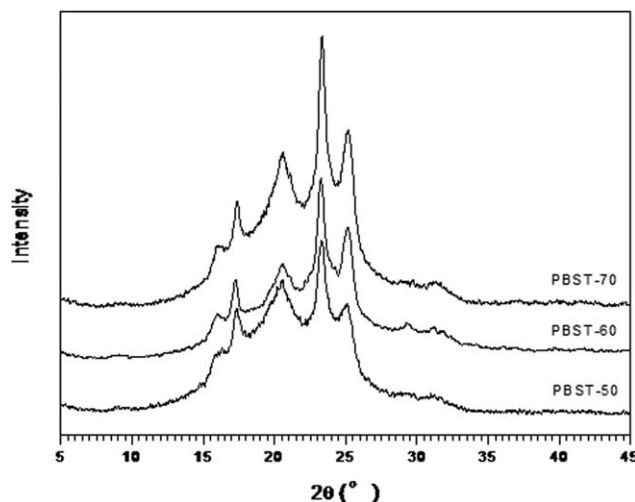


Figure 8 X-ray diffraction patterns of the PBST copolyesters with high BT unit content.

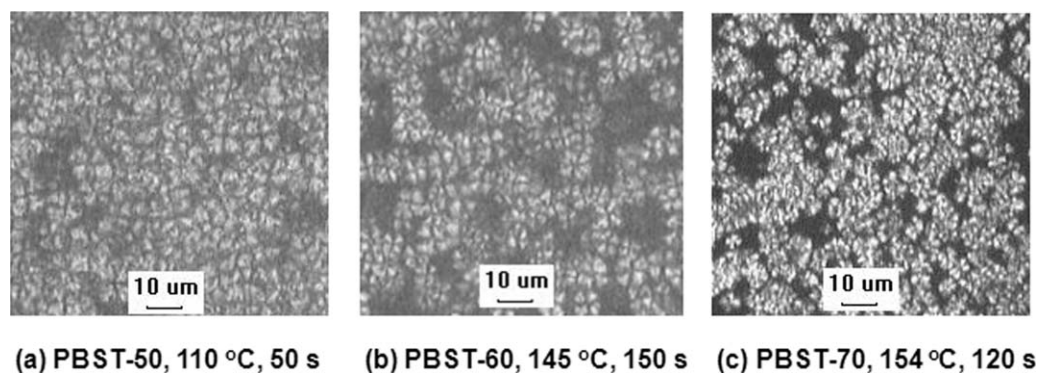


Figure 9 POM micrographs of PBST copolyesters isothermally crystallized at different crystallization temperatures.

crystals that render the three copolyesters melt-spunable into flexible fibers.

CONCLUSIONS

The isothermal crystallization behavior and morphology of PBST copolyesters with high content of BT units were developed and investigated by using DSC, WAXD, SAXS, and POM, respectively. The values of the Avrami exponent n were found within 3.2–4.9, suggesting a three-dimensional growth initiated by homogeneous nucleation mechanism. The overall crystallization activation energy ΔE of the copolyesters increases with the increasing BS unit content, showing that the BS units on the copolyester chain hinder the crystallizability of the BT units. The observed multiple melting peaks of the copolyesters isothermally crystallized at different T_c s are the result of melting–recrystallization process. The melting peak at the lower temperature is attributed to melting of the larger and rougher crystals formed during the isothermal crystallization, while the melting peak at the high temperature results from relatively perfect crystal formed during the recrystallization process.

Based on the Hoffman–Weeks method, the equilibrium melting temperature T_m^0 for samples PBST-50, -60, and -70 is obtained as 173.4, 180.3, and 197.6°C, respectively. However, by using the Gibbs–Thomson method, the three copolyesters have the corresponding T_m^0 s of 176.0, 185.4, and 194.4°C. In consideration of the influences of the second comonomers on the crystal structure of the copolyesters, the latter method is thought to be more reliable. Through WAXD, the three copolyesters have exhibited the same crystal structure as that of PBT polyester, not affected by the incorporation of BS units. The crystals of the three samples are composed of little spherulites observed by POM, the key for being melt-spunable into flexible fibers.

References

- Doi, Y. *Microbial Polyesters*; VCH Publishers: New York, 1990.
- Jérôme, C.; Lecomte, P. *Adv Drug Delivery Rev* 2008, 60, 1056.
- Kubisa, P.; Penczek, S. *Prog Polym Sci* 1999, 24, 1409.
- Gan, Z. H.; Abe, H.; Kurokawa, H.; Doi, Y. *Biomacromolecules* 2001, 2, 605.
- He, Y.; Zhu, B.; Kai, W. H.; Inoue, Y. *Macromolecules* 2004, 37, 3337.
- Yang, J.; Tian, W. S.; Li, Q. B.; Li, Y.; Cao, A. M. *Biomacromolecules* 2004, 5, 2258.
- Shibata, M.; Inoue, Y.; Miyoshi, Y. *Polymer* 2006, 47, 3557.
- Witt, U.; Yamamoto, M.; Seeliger, U.; Müller, R. J.; Warzelhan, V. *Angew Chem Int Ed Engl* 1999, 38, 1438.
- Witt, U.; Müller, R. J.; Deckwer, W. D. *Macromol Chem Phys* 1996, 197, 1525.
- Witt, U.; Müller, R. J.; Deckwer, W. D. *J Macromol Sci Pure Appl Chem* 1995, 32, 851.
- Li, F. X.; Xu, X. J.; Yu, J. Y.; Cao, A. M. *Polym Degrad Stab* 2007, 92, 1053.
- Li, F. X.; Xu, X. J.; Hao, Q. H.; Li, Q. B.; Yu, J. Y.; Cao, A. M. *J Polym Sci Part B: Polym Phys* 2006, 44, 1635.
- Avrami, M. *J Chem Phys* 1939, 7, 1103.
- Avrami, M. *J Chem Phys* 1940, 8, 212.
- Lopez, L. C.; Wilkes, G. *Polymer* 1989, 30, 882.
- Cebe, P.; Hong, S. D. *Polymer* 1986, 27, 1183.
- Yasuniwa, M.; Satou, J. *J Polym Sci Part B: Polym Phys* 2002, 40, 2411.
- Hoffman, J. D.; Weeks, J. J. *J Res Natl Bur Stand* 1962, 66, 13.
- Hoffman, J. D.; Davis, G. T.; Lauritzen, J. I. In *The Rate of Crystallization of Linear Polymers with Chain Folding*, Hannay, N. B., Ed.; Plenum Press: New York, 1976.
- Vonk, C. G. *J Appl Crystallogr* 1973, 6, 148.
- Hoffman, J. D.; Davis, G. T.; Lauritzen, J. I. In *Treatise on Solid State Chemistry*; Hannay, N. B., Ed.; Plenum Press: New York, 1976; Vol 3, Chapter 7.
- Kim, M. H.; Philips, P. J.; Lin, J. S. *J Polym Sci Part B: Polym Phys* 2000, 38, 154.
- Albrecht, T.; Strobl, G. *Macromolecules* 1992, 25, 1752.
- Lotz, B.; Wittmann, J. C. *J Polym Sci Part B: Polym Phys* 1986, 24, 1541.
- Briber, R. M.; Thomas, E. L. *Polymer* 1985, 26, 8.
- Ihn, K. J.; Yoo, E. S.; Im, S. S. *Macromolecules* 1995, 28, 2460.
- Yoshioka, T.; Fujimura, T.; Manabe, N.; Yokota, Y.; Tsuji, M. *Polymer* 2007, 48, 5780.